Experimental Thermal and Fluid Science 90 (2018) 310–318

Contents lists available at ScienceDirect

Experimental Thermal and Fluid Science

journal homepage: www.elsevier.com/locate/etfs

Effects of heat flux, mass flux and channel width on flow boiling performance of porous interconnected microchannel nets

Shiwei Zhang[a], Yalong Sun[a], Wei Yuan[a,*], Yong Tang[a], Heng Tang[a], Kairui Tang[b]

[a] Key Laboratory of Surface Functional Structure Manufacturing of Guangdong Higher Education Institute, South China University of Technology, Guangzhou 510640, China

[b] Mechanical Engineering, Pennsylvania State University, Harrisburg, PA 17057, United States

ARTICLE INFO

Keywords:
Porous interconnected microchannel
Channel width
Flow boiling
Heat transfer
Two-phase instability

ABSTRACT

This study presents an experimental investigation of flow boiling heat transfer performance in porous interconnected microchannel nets (PIMNs) as an effective cooling solution for microelectronic devices. Three PIMNs with different microchannel widths, i.e., 0.25, 0.4 and 0.55 mm, were fabricated via copper powder sintering and wire electric discharge machining. The effects of heat flux, mass flux and channel width on flow boiling characteristics, i.e., two-phase heat transfer, pressure drops and two-phase flow instabilities were evaluated for the optimization design. Flow boiling experiments were conducted using deionized water as the coolant with variation in the heat flux and mass flux of 200–500 kg m^{-2} s^{-1} under an inlet subcooling of 40 K. The high speed visualization showed the flow pattern transition from bubbly flow to annular flow was accompanied with the change of boiling heat transfer mechanisms. Both the heat flux and the mass flux have significant effect on the two-phase heat transfer performance of the PIMNs. The PIMN-2 with the medium channel width of 0.4 mm presented the highest heat transfer coefficients and best capability to mitigate the severe two-phase flow instability, as well as the favorable pressure drop penalty, which achieved the best overall flow boiling performance in this study.

1. Introduction

Microchannel heat sinks, since first introduced by Tuckerman and Pease in 1980s [1], have attracted increasingly worldwide attentions to solve the ever growing cooling demand in critical heat-flux microelectronic devices [2]. Utilizing the two-phase flow boiling of working liquids, they possess the prominent heat dissipation capacity for the compact microelectronics. In the past few decades, various kinds of microchannels have been developed, such as circular [3], rectangular [4], trapezoidal [5], V-grooved [6], diverging/converging [7] shape ones. Besides, microchannels have been applied in other fields [8] and increasing studies [9–12] focus on the micro scale heat transfer.

Although the enhanced heat transfer performance has been reached by the conventional microchannels mentioned above, there are still several unsolved problems which limit their further applications, e.g., the two-phase flow instability [13], the large wall superheat at the onset of nucleate boiling (ONB) [14] and the wall-temperature non-uniformity among the channels [15], etc. Microchannels with reentrant cavities are served as a promising option to address these issues, which have been repeatedly justified by experiments [16–18] and numerical simulations [19–21]. The reentrant cavities facilitate the bubble nucleation as a vapor trap [22], resulting in a significant increase of stable nucleation sites [17] and decrease of flow boiling oscillation [18]. However, most of the previous reports are focused on the reentrant cavities in the sidewall of the main channels, such as with circular [17], offset fan [19], triangular [20] shapes. Other kinds of reentrant structures should also be worthy of comprehensive attention. Recently, Deng et al. [23,24] developed a novel reentrant microchannel with semi-closed Ω-shaped cross section and the flow boiling results showed a significant enhancement of flow boiling heat transfer and mitigation of two-phase flow instabilities.

Besides of the aforementioned advantages possessed by the reentrant microchannels, heat transfer deterioration due to the thickened boundary layer [20] and the bubble clogging [25] is another existent issue, which has aroused intense scholarly interest in the segmented fin structures. Based on the concept of thermal boundary layer redevelopment and generation of secondary flow, a number of segmented structures have been proposed recently, including rectangular fin [26], pin–fin [27,28] and oblique fin [29,30]. Xu et al. [26] conducted numerical simulation of conjugate heat transfer in interrupted

* Corresponding author.
E-mail address: mewyuan@scut.edu.cn (W. Yuan).

http://dx.doi.org/10.1016/j.expthermflusci.2017.10.001
Received 24 March 2017; Received in revised form 20 September 2017; Accepted 1 October 2017
Available online 04 October 2017
0894-1777/

Nomenclature

A_{cl}	total cross section area of the longitudinal channels, m^2
A_t	footprint area of the top surface of the copper block, m^2
CHF	critical heat flux, kW/m^2
C_l	specific heat of working fluid, J/(kg °C)
G	mass flux, $kg\,m^{-2}\,s^{-1}$
h_{fg}	evaporation latent heat of deionized water, J/kg
HTC/h_l	local heat transfer coefficient, $kW\,m^{-2}\,K^{-1}$
IMN	interconnected microchannel net
l_c	distance between the upper surface of copper block to the thermocouples
l_s	thickness of the solder layer, m
L_i	distance from the inlet to thermocouple location in the stream-wise direction, m
L	length of the microchannel, m
$\dot{m}$	mass flow rate, kg/s
ONB	onset of nucleate boiling
PIMN	porous interconnected microchannel net
P_{in}	pressure in the inlet plenum, kPa
P_{out}	pressure in the out plenum, kPa
ΔP	pressure drop, kPa
q_a	actual heat flux supplied to test section, kW/m^2
Q_e	effective heat power supplied to test section, W
Q_n	nominal electric power supplied to test section, W
R_c	thermal conduction resistance of pure copper, °C/m
R_s	thermal conduction resistance of solder, °C/m
R_{total}	total thermal conduction resistance, °C/m
t	time, s
T_{ci}	thermocouple reading, °C
T_{in}	inlet fluid temperature, °C
T_{out}	outlet fluid temperature, °C
$T_{Sat,ci}$	local saturation temperature at the location of thermocouple at the local pressure, °C
T_{wi}	wall temperature, °C
ΔT_{Sat}	wall-superheat, °C
ΔT_{sub}	degree of liquid subcooling, K
$\dot{V}$	volumetric flow rate, m^3/s
φ	heat transfer ratio of the actual heat flux absorbed by the working fluid to the total nominal power input indicated by the wattmeter, q_a/q_n, –
λ_c	thermal conductivity of pure copper, $W\,m^{-1}\,K^{-1}$
λ_s	thermal conductivity of solder, $W\,m^{-1}\,K^{-1}$
x	vapor quality, –
ρ	liquid density, kg/m^3

Subscript

a	actual
c	thermocouple reading
ci	thermocouple location in stream-wise direction
cl	cross section
in	inlet
n	nominal
out	outlet
t	top surface of the copper block
s	solder
sat	saturated
sub	subcooled
w	wall
wi	location on the wall surface in line with the thermocouple

microchannels consisting of a set of separated zones adjoining shortened parallel microchannels and transverse microchambers. The computed hydraulic and thermal boundary layers were redeveloping in each separated zone due to shortened flow length and then the heat transfer significantly enhanced. Law et al. [29] compared the oblique-finned microchannels with the straight-finned microchannels in terms of flow boiling heat transfer and pressure. The continuously developing thin liquid-film in the convective boiling region led to the augmentation of heat transfer and delay of the CHF. Similarly, Prajapati et al. [25] conducted a comparative study between the uniform, diverging and segmented finned microchannels covering a wide range of mass flux and heat flux. The segmented microchannel demonstrated the highest heat transfer coefficient with negligible higher pressure drop compared to other two configurations of channels for the entire range of operating conditions. What' more, the segmented finned geometry completely eliminated the problem of bubble clogging, resulting in smooth and easy passage of growing bubbles.

In order to combine both merits of the reentrant structure and the segmented microchannel, interconnected microchannel nets (IMNs) have been proposed and systematically tested in previous works [31,32]. The IMN features two orthogonally aligned arrays of microchannels on the top and bottom surfaces of the copper substrate. Reentrant square pores are formed at the intersections because of the channel depth exceeding half the substrate thickness and the microchannels are segmented due to the interconnectivity by the backside channels. Therefore, the IMN with the appropriate combination of reentrant and segmented characteristics showed superior performances in the two-phase heat transfer and flow instability mitigation when compared to the conventional rectangular microchannels in the flow boiling experiments [31]. Furthermore, microscale copper particles undergoing the traditional sintering process has been applied to replace the solid substrate in the IMN [33,34]. This porous interconnected microchannel net (PIMN) based on sintered porous media yielded a higher heat transfer coefficient (HTC) and a lower wall superheat at the bubble

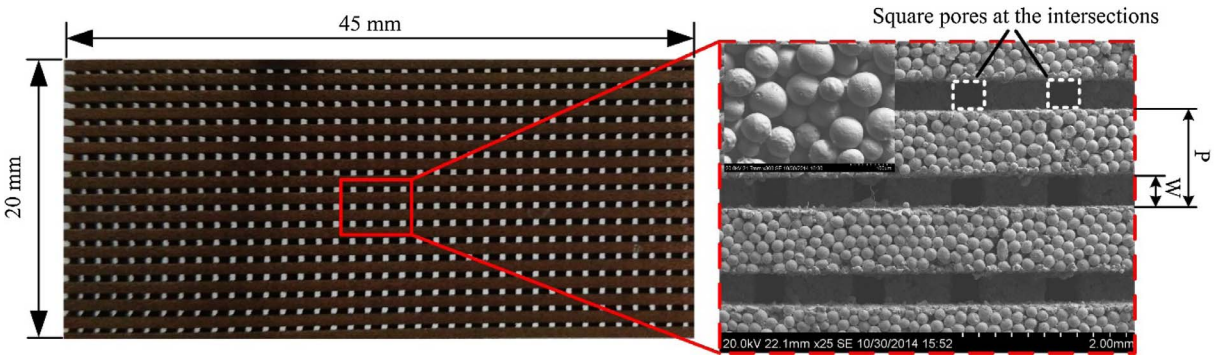

Fig. 1. Profile and SEM of the PIMN.